Least-squares collocation meshless method

Xiong Zhang[*,†], Xiao-Hu Liu, Kang-Zu Song and Ming-Wan Lu

Department of Engineering Mechanics, Tsinghua University, Beijing 100084, People's Republic of China

SUMMARY

A finite point method, least-squares collocation meshless method, is proposed. Except for the collocation points which are used to construct the trial functions, a number of auxiliary points are also adopted. Unlike the direct collocation method, the equilibrium conditions are satisfied not only at the collocation points but also at the auxiliary points in a least-squares sense. The moving least-squares interpolant is used to construct the trial functions. The computational effort required for the present method is in the same order as that required for the direct collocation, while the present method improves the accuracy of solution significantly. The proposed method does not require any mesh so that it is a truly meshless method. Three numerical examples are studied in detail, which show that the proposed method possesses high accuracy with low computational effort. Copyright © 2001 John Wiley & Sons, Ltd.

KEY WORDS: meshless method; moving least-squares; collocation; finite point method

1. INTRODUCTION

The finite element method (FEM) has been the most frequently used numerical method in engineering during the past 30 years. However, the lack of robust and efficient 3D mesh generators makes the solution of 3D problems a difficult task. Furthermore, mesh-based methods are also not well suited to the problems associated with extremely large deformation and problems associated with frequently remeshing. To avoid these drawbacks of the FEM, considerable effort has been devoted during recent years to the development of the so-called meshless method, and about 10 different meshless methods have been developed, such as the smooth particle hydrodynamics (SPH) [1], the element-free Galerkin (EFG) method [2, 3], the reproducing kernel particle (RKP) method [4], the finite point (FP) method [5], the hp clouds method [6], meshless local Petrov–Galerkin (MLPG) [7–10], local boundary integral equation (LBIE) [8–12], and several others [13, 14].

[*]Correspondence to: Xiong Zhang, Department of Engineering Mechanics, Tsinghua University, Beijing 100084, People's Republic of China
[†]E-mail: xzhang@tsinghua.edu.cn

Two methods of discretization, collocation method and Galerkin method, have been domi-
nant in existing meshless methods. Although Galerkin methods possesses several advantages,
one of the major difficulties in the implementation of Galerkin-based meshless methods is
the non-interpolatory character of the approximation. As a consequence, the imposition of
essential boundary conditions is quite awkward and several approaches have been developed
[15–20]. Furthermore, in many Galerkin-based meshless methods, recourse must be taken
to meshes for the purpose of quadrature, so they are not truly meshless methods. In con-
trast, collocation-based meshless methods are truly meshless methods, and are very efficient.
However, equilibrium conditions are satisfied only at collocation points in collocation-based
meshless methods so that significant error could result.

A finite point method, least-squares collocation meshless (LSCM) method, is proposed
in this paper. The moving least-squares interpolant is used to construct the trial functions.
Except for the collocation points which are used to construct the trial functions, a number of
auxiliary points are also used. Unlike the direct collocation method, the equilibrium conditions
are satisfied not only at the collocation points but also at the auxiliary points in a least-
squares sense. The computational effort required for the present method is in the same order
as that required for the direct collocation, while the present method significantly improves the
accuracy of solution. Meanwhile, the present method does not require any mesh so that it is
a truly meshless method. To evaluate the accuracy of the proposed method, three numerical
examples are studied in detail, and numerical results show that the proposed method possesses
high accuracy with low computational effort.

2. WEIGHTED RESIDUAL METHOD

Let us assume a scalar problem governed by a differential equation:

$$A(u) = b \quad \text{in } \Omega \tag{1}$$

with Neumann boundary conditions

$$B(u) = t \quad \text{in } \Gamma_t \tag{2}$$

and Dirichlet (essential) boundary conditions

$$u - u_p = 0 \quad \text{on } \Gamma_u \tag{3}$$

to be satisfied in a domain Ω with boundary $\Gamma = \Gamma_t \cup \Gamma_u$. In the above, A and B are the
appropriate differential operators, u is the problem unknown, u_p is the prescribed value of u
over the boundary Γ_u, and b and t represent external forces or sources acting over the domain
Ω and along the boundary Γ_t, respectively.

The weighted residual method is the most general procedure for solving numerically the
above equations, in which the unknown function u is approximated by some trial approxima-
tion $\hat{u}$, and (1) and (2) are replaced by [5]

$$\int_\Omega W_i(A(\hat{u}) - b) \, d\Omega + \int_{\Gamma_t} \hat{W}_i(B(\hat{u}) - t) \, d\Gamma + \int_{\Gamma_u} \bar{W}_i(\hat{u} - u_p) \, d\Gamma = 0 \tag{4}$$

with the weighting functions $W_i, \bar{W}_i, \hat{W}_i$ defined in different ways.

In order to keep a local character of the problem, function $u(\mathbf{x})$ must be approximated by a combination of locally defined functions as

$$\hat{u}(\mathbf{x}) = \sum_{k=1}^{n_\mathrm{p}} N_k(\mathbf{x})u_k^h = \mathbf{N}^\mathrm{T}(\mathbf{x})\mathbf{u}^h \tag{5}$$

with n_p being the total number of points in the domain and the interpolation functions $N_k(\mathbf{x})$ satisfy

$$N_k(\mathbf{x}) \neq 0 \quad \text{if } \mathbf{x} \in \Omega_k$$

$$N_k(\mathbf{x}) = 0 \quad \text{if } \mathbf{x} \notin \Omega_k \tag{6}$$

where Ω_k is a subdomain of Ω containing n points, $n \ll n_\mathrm{p}$. In (5), u_k^h is the approximate value of u at point k.

3. MOVING LEAST-SQUARES APPROXIMATION

The most frequently used approximation in meshless methods is the moving least-squares interpolant in which the unknown function u is approximated by [2, 3]

$$\hat{u}(\mathbf{x}) = \sum_{i=1}^{m} p_i(\mathbf{x})a_i(\mathbf{x}) = \mathbf{p}^\mathrm{T}(\mathbf{x})\mathbf{a}(\mathbf{x}) \tag{7}$$

where $\mathbf{a}(\mathbf{x})$ is the vector of coefficients, $\mathbf{p}(\mathbf{x})$ is a polynomial basis in the space co-ordinates, and m is the total number of the terms in the basis. For a 2D problem we can specify $\mathbf{p} = [1, x, y]^\mathrm{T}$ for $m = 3$ and $\mathbf{p} = [1, x, y, x^2, xy, y^2]^\mathrm{T}$ for $m = 6$, etc. In (7), $\mathbf{a}(\mathbf{x})$ can be obtained by minimizing a weighted discrete L_2 norm as follows:

$$J = \sum_{j=1}^{n} w_j(\mathbf{x} - \mathbf{x}_j)\big(\mathbf{p}^\mathrm{T}(\mathbf{x}_j)\mathbf{a}(\mathbf{x}) - u_j^h\big)^2 \tag{8}$$

The weight function $w_j(\mathbf{x} - \mathbf{x}_j)$ is usually built in such a way that it takes a unit value in the vicinity of the point j where the function and its derivatives are to be computed and vanishes outside a region Ω_j surrounding the point $\mathbf{x}_j$. A typical choice for $w_j(\mathbf{x} - \mathbf{x}_j)$ is the normalized Gaussian function, namely

$$w_j(r) = \begin{cases} \dfrac{\mathrm{e}^{-(r/c)^2} - \mathrm{e}^{-(d/c)^2}}{1 - \mathrm{e}^{-(d/c)^2}} & r \leqslant d \\ \qquad 0 & r > d \end{cases} \tag{9}$$

where $r = \|\mathbf{x} - \mathbf{x}_j\|$, c is a constant, and d is the size of the influence domain of point $\mathbf{x}_j$.
Minimization of (8) leads to

$$\hat{u}(\mathbf{x}) = \mathbf{p}^\mathrm{T}(\mathbf{x})\mathbf{A}^{-1}(\mathbf{x})\mathbf{B}(\mathbf{x})\mathbf{u}^h \tag{10}$$

where

$$\mathbf{A}(\mathbf{x}) = \sum_{j=1}^{n} w_j(\mathbf{x} - \mathbf{x}_j) \mathbf{p}(\mathbf{x}_j) \mathbf{p}^T(\mathbf{x}_j)$$

(11)

$$\mathbf{B}(\mathbf{x}) = [w_1(\mathbf{x} - \mathbf{x}_1)\mathbf{p}(\mathbf{x}_1), w_2(\mathbf{x} - \mathbf{x}_2)\mathbf{p}(\mathbf{x}_2), \ldots, w_n(\mathbf{x} - \mathbf{x}_n)\mathbf{p}(\mathbf{x}_n)]$$

Comparing (5) and (10) gives

$$\mathbf{N}^T(\mathbf{x}) = \mathbf{p}^T(\mathbf{x})\mathbf{A}^{-1}(\mathbf{x})\mathbf{B}(\mathbf{x})$$

(12)

4. COLLOCATION METHOD

Let $W_i = \hat{W}_i = \bar{W}_i = \delta_i$, where δ_i is the Dirac δ function, Equation (4) gives

$$A(\hat{u}_i) = b_i \quad i = 1, 2, \ldots, n_\Omega$$

$$B(\hat{u}_i) = t_i \quad i = 1, 2, \ldots, n_t$$

(13)

$$\hat{u}_i = u_{pi} \quad i = 1, 2, \ldots, n_u$$

where n_Ω is the total number of points collocated within the domain Ω, n_t the total number of points collocated on the boundary Γ_t and n_u the total number of points collocated on the boundary Γ_u. The above equation may be written in a matrix form as

$$\mathbf{Ku} = \mathbf{f}$$

(14)

where $\mathbf{K}$ is a $n_p \times n_p$ matrix assembled by $A(N_k(\mathbf{x}))$, $B(N_k(\mathbf{x}))$, and $N_k(\mathbf{x})$, $\mathbf{u}$ is the unknown vector consisting of u_k^h ($k = 1, 2, \ldots, n_p$), and $\mathbf{f}$ is the unknown vector assembled by b_i, t_i and u_{pi}.

Meshless methods based on collocation are truly meshless methods, and are very efficient. However, in collocation-based methods, equilibrium conditions are only satisfied at n_Ω collocation points within the domain Ω, and not satisfied elsewhere. If sufficient points are not collocated within the domain Ω, significant error may result. In Galerkin-based methods, equilibrium conditions are satisfied within the domain Ω in an integral sense so that information at Gauss quadrature points are included. Usually, the accuracy of Galerkin-based methods is better than that of collocation-based methods, but the computational effort required for Galerkin-based methods is also much more than that required for collocation-based methods. Taking these points into account, a finite point method is developed based on the least-squares collocation method.

5. LEAST-SQUARES COLLOCATION METHOD

Similar to the direct collocation method, $n_p = n_\Omega + n_t + n_u$ points are collocated in the least-squares collocation method to construct the approximation function $\hat{u}(\mathbf{x})$ for the unknown function $u(\mathbf{x})$ via the moving least-squares approximation. In addition to these n_p collocation points, other n_a auxiliary points are also collocated within the domain Ω. Equilibrium

conditions are satisfied not only at n_p collocation points but also at n_a auxiliary points in a least-squares sense, while boundary conditions are satisfied exactly at $n_t + n_u$ points collocated on the boundaries Γ_t and Γ_u. Compared with the direct collocation method, the total number of unknowns are the same, and the computational effort required for the least-squares collocation method is in the same order as that required for the direct collocation method, while the accuracy is improved significantly.

The equations for the least-squares collocation method may be written as

$$A(\hat{u}_i) = b_i \quad i = 1, 2, \ldots, n_p + n_a$$

$$B(\hat{u}_i) = t_i \quad i = 1, 2, \ldots, n_t \tag{15}$$

$$\hat{u}_i = u_{pi} \quad i = 1, 2, \ldots, n_u$$

Note that the total number of the unknowns in (15) equals n_p, and the total number of the equations equals $n_p + n_a + n_t + n_u$. Consequently, the above equation has to be solved by using the least-squares method. To achieve the best accuracy, the boundary conditions must be satisfied exactly, instead of in a least-squares sense. Rearrange the order of equations in (15) in such a way that the above equation can be rewritten as

$$\begin{bmatrix} \mathbf{K}_{11} & \mathbf{K}_{12} \\ \mathbf{K}_{21} & \mathbf{K}_{22} \end{bmatrix} \cdot \begin{Bmatrix} \mathbf{u}_1 \\ \mathbf{u}_2 \end{Bmatrix} = \begin{Bmatrix} \mathbf{F}_1 \\ \mathbf{F}_2 \end{Bmatrix} \tag{16}$$

where $\mathbf{u}_1$ is the vector of unknowns corresponding to the $n_t + n_u$ points collocated on the boundaries Γ_t and Γ_u, while $\mathbf{u}_2$ the vector of unknowns corresponding to the n_Ω points collocated within the domain Ω. The first row of the above equation is corresponding to the boundary conditions, while the second row is corresponding to the equilibrium conditions. The above equation can be rewritten as

$$\mathbf{K}_{11}\mathbf{u}_1 + \mathbf{K}_{12}\mathbf{u}_2 = \mathbf{F}_1 \tag{17}$$

$$\mathbf{K}_{21}\mathbf{u}_1 + \mathbf{K}_{22}\mathbf{u}_2 = \mathbf{F}_2 \tag{18}$$

Solving (17) for $\mathbf{u}_1$ leads to

$$\mathbf{u}_1 = \mathbf{K}_{11}^{-1}(\mathbf{F}_1 - \mathbf{K}_{12}\mathbf{u}_2) \tag{19}$$

Substituting (19) into (18) results in

$$\mathbf{K}'\mathbf{u}_2 = \mathbf{F}' \tag{20}$$

where $\mathbf{K}' = \mathbf{K}_{22} - \mathbf{K}_{21}\mathbf{K}_{11}^{-1}\mathbf{K}_{12}$, $\mathbf{F}' = \mathbf{F}_2 - \mathbf{K}_{21}\mathbf{K}_{11}^{-1}\mathbf{F}_1$. Equation (20) is a linear least-squares system which can be solved by using several efficient public domain packages, such as *LA-PACK* [22]. After solving (20) for $\mathbf{u}_2$, $\mathbf{u}_1$ can be obtained by solving (19). In (20), there are $n_p + n_a$ equations and only n_Ω unknowns, so it needs to be solved by using the least-squares method. In this sense, the method proposed in this paper is called the least-squares collocation meshless (LSCM) method. The boundary conditions are satisfied exactly at $n_t + n_u$ points collocated on the boundaries Γ_t and Γ_u, while the equilibrium conditions are satisfied at all points in a least-squares sense.

In the proposed method, no mesh is required, so it is a truly meshless method. Because the information at n_a auxiliary points is included, the accuracy of the proposed method is much better than that of the direct collocation method.

6. NUMERICAL EXAMPLES

In this section, n_p represents the total number of collocation points, and n_a represents the total number of auxiliary points. To illustrate the accuracy and efficiency of the proposed method, three cases are analyzed in every numerical example. The first and second cases are analyzed by using the direct collocation method, while the third case is analyzed by using the proposed method. The approximation function $\hat{u}$ is constructed via the n_p collocation points in the first case, and is constructed via both the n_p collocation points and n_a auxiliary points in the second case. Consequently, the number of degree of freedom equals n_p in the first and third cases, and equals $n_p + n_a$ in the second case.

6.1. Poisson equation

As the first numerical example, the Poisson equation,

$$\Delta u(x, y) = -2(x + y - x^2 - y^2) \quad \text{in } \Omega : x \in [0, 1], \ y \in [0, 1]$$

$$u(x, y) = 0.0 \quad \text{on } \partial\Omega \tag{21}$$

is studied. The exact solution is given by

$$u(x, y) = (x - x^2)(y - y^2)$$

Nodes discretization is shown in Figure 1, in which the solid circles indicate the collocation points, and the hollow circles indicate the auxiliary points. Figure 2 compares numerical results obtained by different methods at stations along $x = 0.35$.

To compare the computational effort required for the different collocation schemes, the problem is analyzed in a PII 266 computer by using a regular discretization as shown in Figure 3. The numerical results obtained by the three collocation schemes are shown in Figure 4, which are very close to the exact solution. The computational time required is listed in Table I, which shows that the proposed method is much more efficient than direct collocation.

6.2. Cantilever beam

The exact solution for cantilever beam subjected to end load as shown in Figure 5 is given by Timoshenko and Goodier [21] as

$$u_x = -\frac{P}{6EI}\left(y - \frac{D}{2}\right)\left[(6L - 3x)x + (2 + v)(y^2 - Dy)\right]$$

$$u_y = \frac{P}{6EI}\left[3v\left(y - \frac{1}{2}D\right)^2(L - x) + \frac{1}{4}(4 + 5v)D^2x + (3L - x)x^2\right] \tag{22}$$
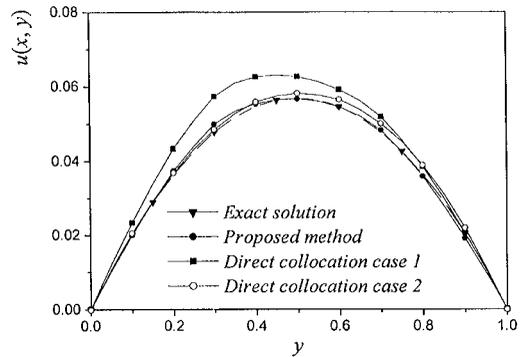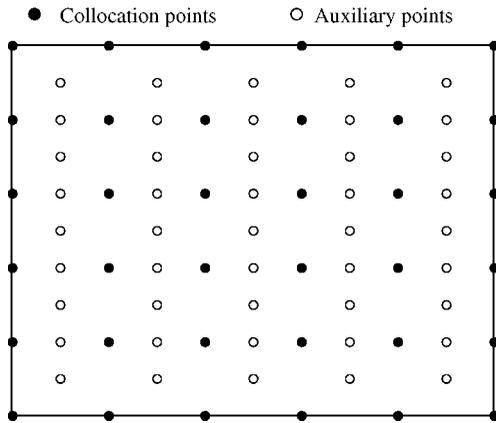
Figure 1. Nodal arrangement ($n_p = 36, n_a = 36$).

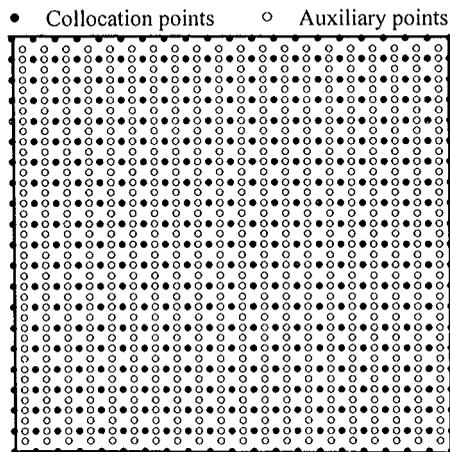Figure 2. Results comparison at stations along $x = 0.35$.

Figure 3. Regular nodal discretization ($n_p = 441, n_a = 780$).

where E is the elastic modulus, v is the Poisson's ratio, and I is the moment of inertia which is given by $D^3/12$ for a beam with rectangular cross-section and unit thickness. The stresses are given by

$$\sigma_{xx} = -\frac{P}{I}(L - x)\left(y - \frac{1}{2}D\right)$$

$$\sigma_{yy} = 0 \qquad\qquad (23)$$

$$\sigma_{xy} = -\frac{Py}{2I}(y - D)$$

Int. J. Numer. Meth. Engng 2001; **51**:1089–1100
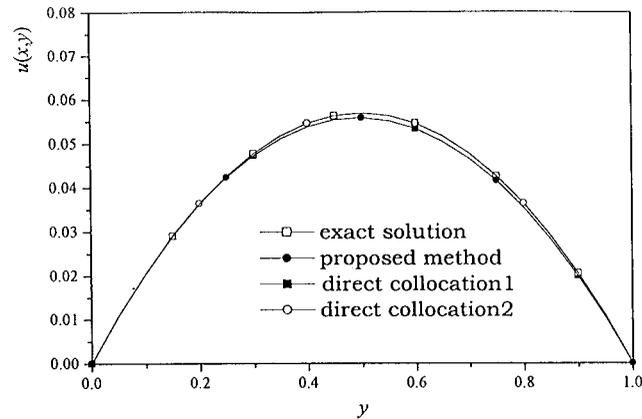
Figure 4. Numerical results obtained by using different collocation schemes at stations along $x = 0.35$.

Table I. Computational time required (s).

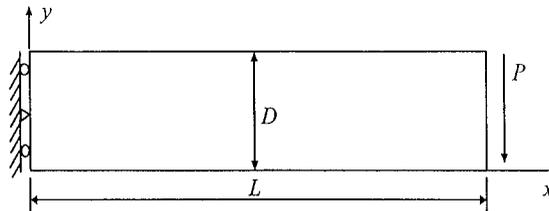| Collocation scheme	DC case 1	DC case 2	Least-squares collocation
CPU time required	6	33	14

Figure 5. A cantilever beam.

This problem is analyzed with dimensionless parameters $E = 1.0 \times 10^3$, $v = \frac{1}{3}$, $P = 1$, $D = 2$ and $L = 12$. Nodal arrangement for this analysis is shown in Figure 6. Figure 7 compares the stress σ_x at the stations along upper surface of the beam obtained by using the present method with those obtained by using the direct collocation method, and it shows that the present method gives much better results than those given by the direct collocation method.

Numerical results for case 1 show a clear instability, which is typical in point collocation procedures. To investigate if the proposed method is free of these instabilities, the cantilever beam is analyzed again by using the node discretization as shown in Figure 8. The numerical results obtained by using the proposed method are compared with those obtained by using direct collocations in Figure 9, which shows again that the proposed method is still stable, while the direct collocations are unstable. Due to lack of sufficient study, the proposed method cannot be guaranteed to be stable in any case, but it can be concluded that the proposed method performs much better than the direct collocation.
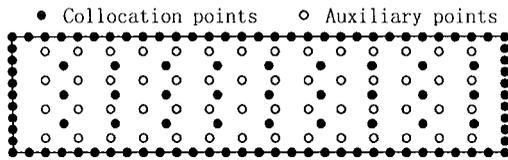
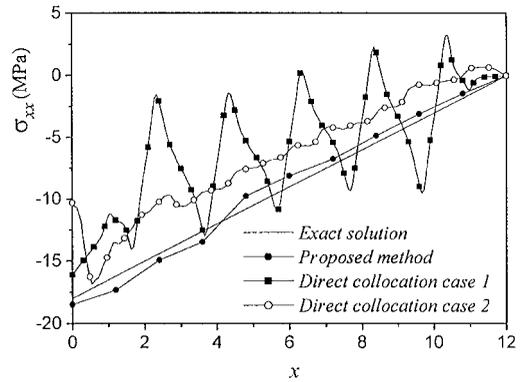Figure 6. Nodal arrangement of the cantilever beam ($n_p = 107, n_a = 64$).

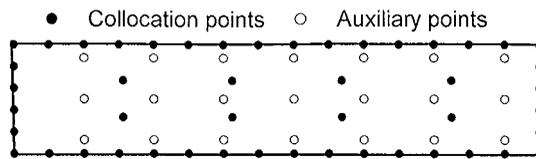Figure 7. Stress σ_{xx} at stations along upper surface of the beam.

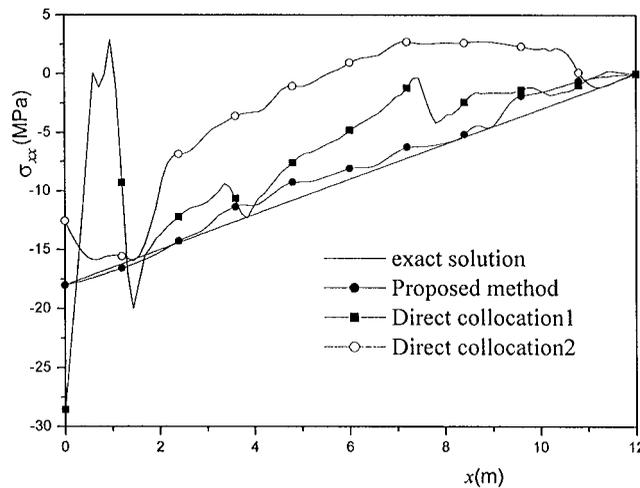Figure 8. Node discretization ($n_p = 48, n_a = 21$).

Figure 9. Stress σ_{xx} at stations along upper surface of the beam obtained by using different collocation schemes.

6.3. *An infinite plate with hole*

Consider the problem of an infinite plate with a hole of radius a loaded at infinity by a traction σ_0 in the x direction. The analytical solution of this problem is given by

$$\sigma_x(x, y) = \sigma_0 \left\{ 1 - \frac{a^2}{r^2} \left(\frac{3}{2} \cos 2\theta + \cos 4\theta \right) + \frac{3a^4}{2r^4} \cos 4\theta \right\}$$

$$\sigma_y(x, y) = -\sigma_0 \left\{ \frac{a^2}{r^2} \left(\frac{1}{2} \cos 2\theta - \cos 4\theta \right) - \frac{3a^4}{2r^4} \cos 4\theta \right\} \tag{24}$$

$$\tau_{xy}(x, y) = -\sigma_0 \left\{ \frac{a^2}{r^2} \left(\frac{1}{2} \sin 2\theta + \sin 4\theta \right) + \frac{3a^4}{2r^4} \sin 4\theta \right\}$$

$$u_r = \frac{\sigma_0}{4G} \left\{ r \left[\frac{\kappa - 1}{2} + \cos 2\theta \right] + \frac{a^2}{r} [1 + (1 + \kappa) \cos 2\theta] - \frac{a^4}{r^3} \cos 2\theta \right\}$$

$$u_\theta = \frac{\sigma_0}{4G} \left\{ (1 - \kappa) \frac{a^2}{r} - r - \frac{a^4}{r^3} \right\} \sin 2\theta \tag{25}$$

where

$$G = \frac{E}{2(1 + v)}, \quad \kappa = \begin{cases} 3 - 4v & \text{plane strain} \\ \dfrac{3 - v}{1 + v} & \text{plane stress} \end{cases}$$

and (r, θ) is a polar co-ordinate system with the origin at the centre of the hole.

Due to symmetry, only the upper right quadrant of the plate is modelled. A plane stress state is assumed with dimensionless elastic modulus $E = 1 \times 10^3$ and Poisson's ratio $v = 0.3$. σ_0 is assumed to be 1. Symmetry conditions are imposed on the left and bottom edges, and the inner boundary at $a = 1$ is traction free. Tractions corresponding to the analytical solution (24) are prescribed at the right and upper boundary, so that the problem analyzed is an infinite plate with a central circular hole. Nodal arrangement is shown in Figure 10, and the stresses σ_{xx} at stations along the left edge are compared with those obtained by the direct collocation method in Figure 11.

7. CONCLUDING REMARKS

A finite point method, least-squares collocation meshless method, is developed in this paper. The total number of unknowns in the present method equals that in direct collocation method, so that the present method does not increase the computational effort significantly. However, the present method improves the accuracy of the solution significantly, as illustrated in the above numerical examples. Furthermore, the present method does not require any mesh, so it is a truly meshless method. Numerical studies show that the proposed method performs much better than the direct collocations.
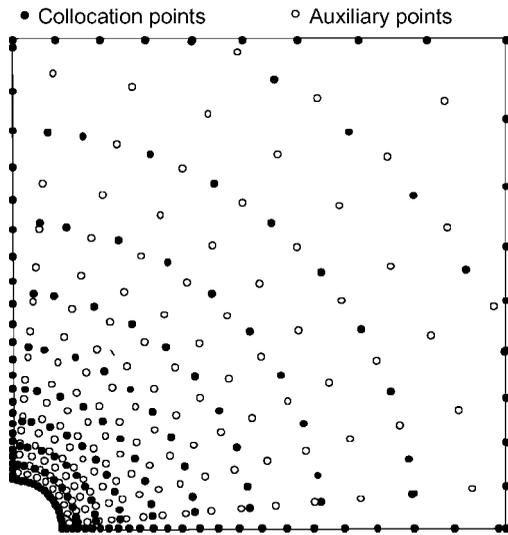
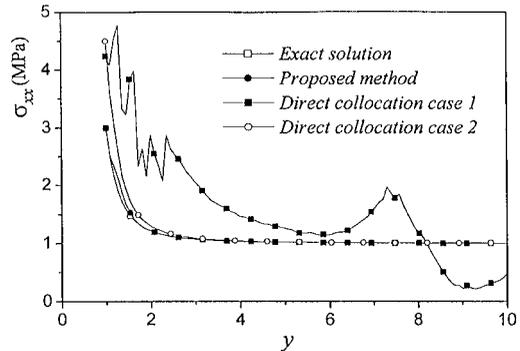Figure 10. Nodal arrangement of the plate $(n_p = 172, n_a = 150)$.

Figure 11. Stress σ_{xx} at stations along left edge.

REFERENCES

1. Gingold RA, Moraghan JJ. Smoothed particle hydrodynamics: theory and applications to non-spherical stars. *Monthly Notices of the Royal Astronomical Society* 1977; **181**:375–389.
2. Belytschko T, Lu Y, Gu L. Element free Galerkin methods. *International Journal for Numerical Methods in Engineering* 1994; **37**:229–256.
3. Belytschko T, Krongauz Y, Organ D *et al*. Meshless methods: An overview and recent developments. *Computer Methods in Applied Mechanics and Engineering* 1996; **139**:3–47.
4. Liu WK, Jun S, Zhang YF. Reproducing kernel particle methods. *International Journal for Numerical Methods in Fluids* 1995; **20**:1081–1106.
5. Oñate E, Idelsohn S, Zienkiewicz OC, Taylor RL. A finite point method in computational mechanics. Applications to convective transport and fluid flow. *International Journal for Numerical Methods in Engineering* 1996; **39**(22):3839–3866.
6. Liszka TJ, Duarte CAM, Tworzydlo WW. hp-meshless cloud method. *Computer Methods in Applied Mechanics and Engineering* 1996; **139**:263–288.
7. Atluri SN, Zhu TL. The meshless local Petrov–Galerkin (MLPG) approach for solving problems in elasto-statics. *Computational Mechanics* 2000; **25**:169–179.
8. Atluri SN, Zhu TL. New concepts in meshless methods. *International Journal for Numerical Methods in Engineering* 2000; **47**(1–3):537–556.
9. Atluri SN, Kim HG *et al*. A critical assessment of the truly meshless local Petrov–Galerkin (MLPG), and local boundary integral equation (LBIE) methods. *Computational Mechanics* 1999; **24**:348–372.
10. Atluri SN, Zhu T. A new meshless local Petrov–Galerkin (MLPG) approach in computational mechanics. *Computational Mechanics* 1998; **22**:117–127.
11. Atluri SN, Sladek J *et al*. The local boundary integral equation (LBIE) and it's meshless implementation for linear elasticity. *Computational Mechanics* 2000; **25**:180–198.
12. Zhu T, Zhang JD, Atluri SN. A local boundary integral equation (LBIE) method in computational mechanics, and a meshless discretization approach. *Computational Mechanics* 1998; **21**:223–235.
13. Zhang X, Lu MW, Wegner JL. A 2-D meshless model for jointed rock structures. *International Journal for Numerical Methods in Engineering* 2000; **47**(10):1649–1661.
14. Zhang X, Song KZ, Lu MW. Meshless methods based on collocation with radial basis functions. *Computational Mechanics* 2000; **26**(4):333–343.
15. Krongauz Y, Belytschko T. Enforcement of essential boundary conditions in meshless approximations using finite elements. *Computer Methods in Applied Mechanics and Engineering* 1996; **131**:133–145.

16. Lu YY, Belytschko T, Gu L. A new implementation of the element free Galerkin method. *Computer Methods in Applied Mechanics and Engineering* 1994; **113**:397–414.
17. Gosz J, Liu WK. Admissible approximations for essential boundary conditions in the reproducing kernel particle method. *Computational Mechanics* 1996; **19**:120–135.
18. Zhu T, Atluri SN. Modified collocation method and a penalty formulation for enforcing the essential boundary conditions in the element free Galerkin method. *Computational Mechanics* 1998; **21**:211–222.
19. Mukherjee YX, Mukherjee S. On boundary conditions in the element free Galerkin method. *Computational Mechanics* 1997; **19**:267–270.
20. Zhang X, Liu X, Lu MW, Chen Y. Imposition of essential boundary conditions by displacement constraint equations in meshless methods. *Communications in Numerical Methods in Engineering*, in press.
21. Timoshenko SP, Goodier JN. *Theory of Elasticity*, 3rd (edn). McGraw-Hill: New York, 1987.
22. Anderson E, Bai Z *et al*. *LAPACK Users' Guide*. Society for Industrial and Applied Mathematics: Philadelphia, PA, 1992.